

Plasma modification of polymeric single end cords as an alternative to RFL treatment

A. Louis, J.W.M. Noordermeer, W.K. Dierkes\*, A. Blume  
Department of Elastomer Technology and Engineering, University of Twente,  
P.O. Box 217, 7500AE Enschede, the Netherlands

Presented at the Fall 192nd Technical  
Meeting of Rubber Division, ACS  
Cleveland, OH  
October 10-12,  
2017

ISSN: 1547-1977

\* Speaker

## ABSTRACT

Adhesion between reinforcing fibers and a matrix is crucial for good performance of a wide variety of elastomeric products. RFL treatment is still and was the most commonly used technology to achieve rubber-fiber adhesion for decades; however, there are health concerns related to this method. Therefore, alternative technologies to partly or completely replace the RFL treatment are currently developed.

A new approach for adhesion enhancement is plasma treatment of fibers/cords. This process allows to physically and chemically modify the cord surface and thus to increase compatibility with and reactivity towards the elastomeric matrix.

In this study, an atmospheric plasma jet was used to coat polymeric cord surfaces with an adhesive layer on a pilot-scale continuously operating line. The precursors used for the chemical surface modification of the cords carried sulfuric moieties and/or unsaturated carbon-carbon bonds, to result in functional groups reactive towards the polymer after the plasma polymerization and deposition on the cord surface. The crucial components of the equipment, process parameters, and pre- as well as post-treatments were elaborated. The results in terms of cord properties as well as adhesion strength of the cords to an elastomeric compound will be discussed.

## INTRODUCTION

A novel route of creating an adhesive layer on a cord surface, which is responsive towards rubber, is explored. The basic concept is the application of a plasma polymerization process to create such a layer with the aid of a precursor, which splits up into radicals in the plasma and undergoes a polymerization reaction during the deposition onto the cord surface.

The novelty of this process is the use of precursors applied to polymeric cords in an atmospheric pressure plasma reactor under protective atmosphere. Usually, the plasma technique is used to enhance the surface energy and polarity in order to make a surface more reactive for adhesive applications, or for simple cleaning purposes.

Besides the possibility of in-line processing, plasma polymerization at atmospheric pressure has some other advantages over deposition at low pressures. Since the chance that gas molecules collide is significantly higher at atmospheric pressure than in vacuum, energy transfer is more efficient. In vacuum, the monomer molecules are often fragmented by the collision with the high-energetic plasma species. The lower energy of plasma species at atmospheric pressure results in a better retention of the chemical structure. Furthermore, the higher monomer concentration at atmospheric pressure results in a higher deposition yield.

Sulfur-containing precursors are chosen in order to generate a plasma coating that has the ability to interact with the sulfur accelerator complexes which are formed during the vulcanization of rubber. A number of molecules were considered for such an application: polysulfides may function as a sulfur donor or enhance the chance of interaction with the accelerator complexes. Furthermore, the combination with other functional groups can be of interest, as the molecule may reconfigure during the exposure to the plasma or interact with plasma radicals.

Thiophene ( $C_4H_4S$ ) features a five membered ring structure of four carbons and one sulfur atom, with two double bonds (see Figure 1). The ring structure gives the molecule a certain stability when exposed to plasma. Similar to pyrrole, thiophene is well known to polymerize under plasma conditions to polythiophene. This polymer can be electrically conductive; however, plasma polymerization does in general not form polymers with a high stereoregularity.

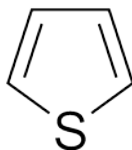


Figure 1: Thiophene

Diallyl disulfide ( $C_6H_{10}S_2$ ), see Fig. 2, provides double bonds as well as a disulfide moiety. However, this molecule doesn't offer a ring structure which may make it rather vulnerable in the plasma and it is unlikely that it forms a proper polymer. It is more likely that it might plasma-polymerize but won't form polymer chains of a proper length and regularity. However, diallyl disulfide should be relatively easy to activate and should therefore require a low energy input. The sulfur-sulfur bond is particularly weak with a bond energy of 2.3 eV [1], this implies that it is likely that the molecule will split easily. The carbon-carbon double bonds are located at the end of the molecule, so they do not contribute to a stable ring-structure like in thiophene. If the molecule splits at the sulfur-sulfur bond in the plasma, it could happen that the double bond and the sulfur radical both react with the cord surface. Another shortcoming is that diallyl disulfide is in fact condensed garlic liquid, it has a quite distinctive smell at very small concentrations.

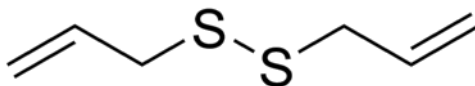


Figure 2: Diallyl disulfide

Dibenzyl disulfide ( $C_{14}H_{14}S_2$ ), shown in Fig. 3, is another disulfide that has a similar structure but differs in its functional end groups. Instead of double bonds it features aromatic rings. These rings can get opened by the plasma and can undergo radical reactions with the cord surface. A plasma polymerization that forms a certain regular structure like in the case of thiophene is not to be expected. However, plasma can create fragments of this molecule which then recombine to structures that have a higher molecular weight and are also attached to the cord surface.

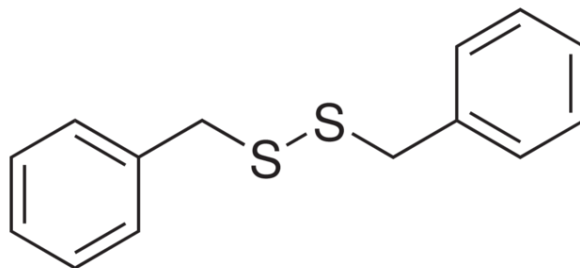


Figure 3: Dibenzyl disulfide

Dimethyl trisulfide ( $C_2H_6S_3$ ), see Fig. 4, is basically a chain of three sulfur atoms with methyl groups attached at each end. A common abbreviation is DMTS. It is missing the double bonds present in the other molecules, though due to the plasma activation of the cord and the molecule itself, a chemical bond of the deposited layer with the cord is possible. Similar to the diallyl disulfide discussed before, this trisulfide features no ring structure and that makes it vulnerable within the plasma and likely to get fragmented. However, the deposition and recombination process might establish sulfur chains within the deposited layer. As there are no double bonds available, the plasma polymerization of the deposited atoms may form a less regularly structured polymer. However, the increased amount of sulfur might create a high reactivity during vulcanization and therefore result in a good adhesion between rubber and reinforcing cord.

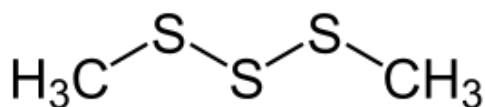


Figure 4: Dimethyl trisulfide

**TABLE I**  
**OVERVIEW OF THE PROPERTIES OF SULFUR PRECURSORS**

| <b>Precursor</b>                 | <b>Thiophene</b>                | <b>Diallyl disulfide</b>                      | <b>Dibenzyl disulfide</b>                      | <b>Dimethyl trisulfide</b>                   |
|----------------------------------|---------------------------------|---|--|--|
| <b>Molecular Formula</b>         | C <sub>4</sub> H <sub>4</sub> S | C <sub>6</sub> H <sub>10</sub> S <sub>2</sub> | C <sub>14</sub> H <sub>14</sub> S <sub>2</sub> | C <sub>2</sub> H <sub>6</sub> S <sub>3</sub> |
| <b>CAS number</b>                | 110-02-1                        | 2179-57-9                                     | 150-60-7                                       | 3658-80-8                                    |
| <b>Molecular weight, g/mol</b>   | 84,14                           | 146,28  | 246,39   | 126,26                                       |
| <b>Density, g/cm<sup>3</sup></b> | 1,06                            | 1,01  | 1,30   | 1,20   |
| <b>Melting point, °C</b>         | -38                             | 79*   | 69-72  | -68  |
| <b>Boiling point, °C</b>         | 84                              | 180   | 210-216  | 170  |
| <b>Hazard symbol</b>             | F, Xn                           | Xn  | Xi   | none   |

\*at 16 mm Hg

With the variation in precursors as shown in Table I it can be deduced if a certain aspect of a molecule is beneficial for the plasma treatment process. For example, if the number of sulfur atoms plays a role in the coatings' ability to interact with sulfur complexes, or if the number of double bonds is a criteria. More than three sulfur atoms in a row in the molecule was considered to be possibly problematic, as the precursor might convert to a lower number of sulfur atoms in its chain by releasing elemental sulfur. This is possible in particular during the evaporation phase and the injection into the plasma. Besides, molecules with aromatic rings are difficult to use, as they usually have a high boiling point that is not feasible with the given setup.

An overview of bond energies is given in Table II. A plasma can atomize a whole molecule which leaves room for recombination in conjunction with surface interactions. The recombination process of a molecule after it was atomized by plasma is not predictable and happens in a random order.

**TABLE II**  
**BOND ENERGIES OF COMMON CARBON AND SULFUR BONDS [1]**

| Bond                  | kJ/mol | eV  | Bond | kJ/mol | eV  |
|-----------------------|--------|-----|------|--------|-----|
| C-C                   | 346    | 3.6 | C=C  | 602    | 6.3 |
| C-O                   | 358    | 3.7 | C=O  | 799    | 8.3 |
| C-S                   | 272    | 2.8 | C=S  | 573    | 6.0 |
| S-S (S <sub>8</sub> ) | 226    | 2.3 | S=S  | 425    | 4.4 |
| C-N                   | 305    | 3.2 | C=N  | 615    | 6.4 |

For comparison, sulfur-less precursors were also used. Pyrrole (C<sub>4</sub>H<sub>5</sub>N), shown in Fig. 5, is, just like thiophene, a heterocyclic aromatic organic compound and structured as a five-membered ring. Unlike thiophene, it has a dipole in which the positive end lies on the side of the heteroatom, with a dipole moment of 1.58 D [2].

Due to its aromatic character, pyrrole is difficult to hydrogenate and has a high p-electron density. It can polymerize under plasma conditions forming polypyrrole (PPy). PPy is an insulator, but its oxidized derivatives are good electrical conductors. The conductivity of the material depends on the conditions and reagents used in the oxidation. Conductivities range  $26.40 \times 10^{-4}$  S/m [3].

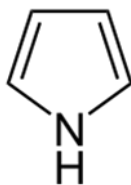


Figure 5: Pyrrole

1,3-Butadiene (C<sub>4</sub>H<sub>6</sub>) has two conjugated double bonds as seen in Fig. 6, and can therefore take part in numerous reactions, which include 1,2- and 1,4-additions with itself (polymerization) and other reagents, linear dimerization and trimerization, and ring formation. The 1,3 isomer is economically the most important unsaturated C<sub>4</sub> hydrocarbon [4].

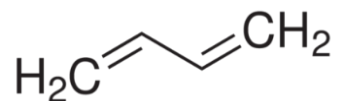


Figure 6: 1,3-butadiene

Tetrahydrothiophene ( $C_4H_8S$ , Fig. 7) is the saturated equivalent of thiophene. It consists of a five-membered ring containing four carbon atoms and a sulfur atom. It is a volatile, colorless liquid with an intensely unpleasant odor. Together with its unsaturated analog and pyrrole it can be used to study the effect of plasma on these different ring-structured molecules.

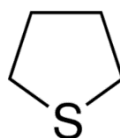


Figure 7: Tetrahydrothiophene

Usually no specific structure results from polymerization in a straightforward manner under plasma conditions, as significant fragmentation and rearrangement of atoms in the original starting material occurs. However, the structure of the monomers largely determines the fragmentation pattern that occurs in the plasma. It is a random process and predictions are not reliable [5]. The ring structures of thiophene and pyrrole are opened up [6], and complete fragmentation will not occur. This way, either polythiophene (PT) or polypyrrole (PPy) can form.

## EXPERIMENTAL

### MATERIALS

Untreated polymeric rayon cords were used. The cord was a 610F Super 2 1840 dtex f1000 x2, which was supplied by Cordenka GmbH & Co. KG, Obernburg, Germany. All precursors were of a purity of >99% and ordered from Sigma Aldrich.

### PLASMA TREATMENT SETUP

The plasma treatment was done in a two-step process: decontamination followed by plasma coating with a precursor. Both steps were performed under nitrogen gas atmosphere, which was



controlled by the visual appearance of the plasma flame. Inside both chambers (see Figure 8), an overpressure of about 0.2 bar was set via controlling the exhaust streams with external valves. The whole treatment line consisted of the following components:

- McCoy Single End Tension Stand Model 21T with load cell tension controller;
- IR heater Mo-El Halogen IR Fiore 1800;
- Plasma cleaning unit (CU) consisting of a Plasmatreat FG1001 plasma generator with two PFW10 plasma nozzles;
- Plasma polymerization unit (PU) based on a Plasmatreat FG5001 plasma generator with two PFW10-PAD plasma nozzles and a plasma polymerization unit PAD1;
- Both plasma units, each installed in a separate cabinet, are attached to an exhaust extraction system by Nederman, which is able to create a low pressure environment inside the cabinets;
- Planetruder S extruder (VMI) with attached crosshead for single-end cord application;
- Computer-controlled winding unit with freely scalable winding speed.

Figure 8 shows the design of the plasma treatment chamber with two sets of Atmospheric Pressure Plasma Jets (APPJ).

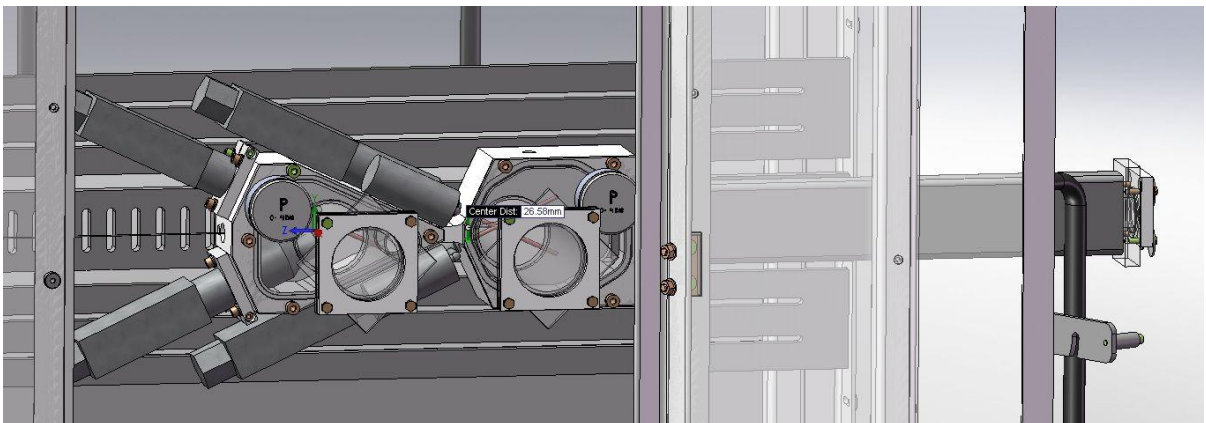


Figure 8: Final CAD design of the overpressure plasma chamber with the four APPJs in place

#### H-PULLOUT TEST

This test method measures adhesion of reinforcing cords bonded to rubber compounds, and is documented in ASTM standard D4776M-10 [7]. It is primarily used to evaluate tire cords, but

can also be used to evaluate tire cord adhesives using one consistent form of tire cord and rubber compound. In this work, each batch was tested 15fold.

#### STRAP PEEL ADHESION FORCE (SPAF) TEST

The SPAF test is the standard test method for strap peel adhesion of reinforcing cords or fabrics to rubber compounds as defined in ASTM D 4393 [8]. The test is performed with a tensile testing machine, which has to fulfill the requirements of ISO 5893, with an accuracy of the force measurement complying to class 2 and a 10 kN load cell. The grippers for holding the test specimen in the testing machine during the measurement correspond to ASTM D 413. Within this test, the force is measured as a function of peel distance. However, the primary information gathered by this test is the degree of rubber coverage, which is expressed as a percentage value judged by the operator. It can be given a value of 100 % coverage, which is equivalent to a failure entirely within the rubber phase in-between the cord layers. If the failure is also partly at the interface, the coverage value can be judged stepwise with 90, 80, 70, 50 or 30 % of coverage.

#### X-RAY PHOTOELECTRON SPECTROSCOPY (XPS)

XPS is a tool for the chemical analysis of a surface layer, of the top 1-10 nm, for any solid substrate. The XPS measurements were performed with a Quantera SXM (scanning XPS microprobe) from Physical Electronics equipped with an Al K $\alpha$  X-ray, which is monochromatic at 1486.6 eV. The working pressure was  $2 \cdot 10^{-8}$  torr and the remaining gas was argon for neutralization. The analysis was done with Compass for XPS control and Multipak v.9.4.0.7 for data reduction. Fitting of spectra was done after shifting of the measured spectra with respect to the known reference binding energies. The samples were taken directly from the plasma treatment process, where they were put into a plastic bag protected by a nitrogen atmosphere and directly transported to the XPS lab. The samples were cut to a suitable size for the XPS vacuum chamber and attached to a sample holder. The sample holder was placed immediately into the XPS and kept under vacuum until the measurement was performed.

#### STEREO MICROSCOPE

A stereo microscope from Leica of the type MZ 125 was used to analyze the plasma treated samples optically. This stereo microscope has a useful magnification of up to 100x. To capture

images, a digital camera, Leica DFC 240 with 3 megapixel, was used and the images were edited, saved and organized with the Leica LAS 3.8 software. As samples, H-pullout specimens after testing were taken. They were cut either rectangular to the cord direction or, if the cord was pulled out from that sample part, cut parallel to the cord direction to monitor the failure interface. Those specimen parts have been reduced in size to an effective dimension of roughly 5 x 5 x 5 mm. Modeling clay has been applied to secure the specimen when placed under the microscope.

## RESULTS AND DISCUSSION

The first stage of the development of the plasma cleaning and coating process was done by a Design of Experiments (DoE) setup. The FG5001 generator allows the configuration of several parameters. These are mainly parameters concerning the generator power itself, the gas pressure and the flow-rates of the precursor. The latter is injected into the plasma in an evaporated state for plasma coating purposes, together with the ionization as well as the carrier gases.

Experience has shown that the gas flow-rates are supposed to have minor effects on the plasma properties and can therefore be kept constant for a DoE setup. The parameters with a major effect (see Table III) on the treatment process were expected to be the voltage settings (in percentage) of the generator, the frequency in kHz of the excitation process and the cycle time, which determines how long the excitation is activated per cycle. Additionally, the flow-rate of the precursor was considered to have a significant effect on the process. The precursor itself was kept constant, and with pyrrole a precursor was chosen known for its ability to plasma polymerize [14].

**TABLE III**  
**SELECTED PLASMA PARAMETERS FOR THE DOE TRIALS**

| <b>Factor</b> | <b>Type</b>     | -  | +   | <b>CP</b> |
|---------------|-----------------|----|-----|-----------|
| <b>A</b>      | Voltage [%]     | 85 | 100 | 92,5      |
| <b>B</b>      | Frequency [kHz] | 19 | 25  | 22        |
| <b>C</b>      | Cycle time [%]  | 50 | 100 | 75        |
| <b>D</b>      | Flow-Rate [g/h] | 20 | 100 | 60        |

The following plasma settings were constant during the DoE trials:

- primary pressure [mbar]: 1000
- flow-rate ionization gas [L/h]: 2074
- flow-rate carrier gas [L/h]: 271
- temperature of evaporator [°C]: 133

All gas related values were kept at the original system settings. The temperature of the evaporator for the precursor was set to a value above the boiling point of pyrrole, which is 129°C.

**TABLE IV**  
**THE DOE SETUP**

| #DoE- | A | B | C | D | Answer |
|-------|---|---|---|---|--------|
| 1     | - | - | - | - | 9,3    |
| 2     | + | - | - | - | 10,4   |
| 3*    | - | + | - | - | -      |
| 4*    | + | + | - | - | -      |
| 5     | - | - | + | - | 9,8    |
| 6     | + | - | + | - | 9,5    |
| 7*    | - | + | + | - | -      |
| 8     | + | + | + | - | 10,1   |
| 9     | - | - | - | + | 9,5    |
| 10    | + | - | - | + | 9,3    |
| 11*   | - | + | - | + | -      |
| 12*   | + | + | - | + | -      |
| 13    | - | - | + | + | 9,8    |
| 14    | + | - | + | + | 10,9   |
| 15    | - | + | + | + | 11,2   |
| 16    | + | + | + | + | 11,6   |
| CP    | 0 | 0 | 0 | 0 | 11,1   |

*\* These parameter settings did not allow plasma ignition.*

The performed trials, which consequently consist of 16 trials plus a center point (CP) test, are documented in Table IV. The answer column reflects the measured H-pullout force values of each sample. A few factor combinations turned out not to be feasible, because the generator was not able to ignite the plasma under these circumstances.

However, the results from this combination of factors are not satisfactory. The fact that the values are all low supports the hypothesis that another factor is responsible for good adhesion. That might be the precursor itself, which might not have formed moieties - double bonds - during the plasma coating which can interact with the sulfur complexes during vulcanization. In this case, the coating would make the cord even more inert, what subsequently prevented any development of adhesive forces between coating and rubber. Another possible explanation is that the freshly plasma treated cord surface reacted with the surrounding air in a way that the top-layer got oxidized, which made the surface more polar and blocked the interaction between coating and rubber.

To better understand what happened to the cord surface after the plasma coating, four samples with either strong or weak plasma settings and either high or low flow-rates were chosen to be analyzed by XPS.

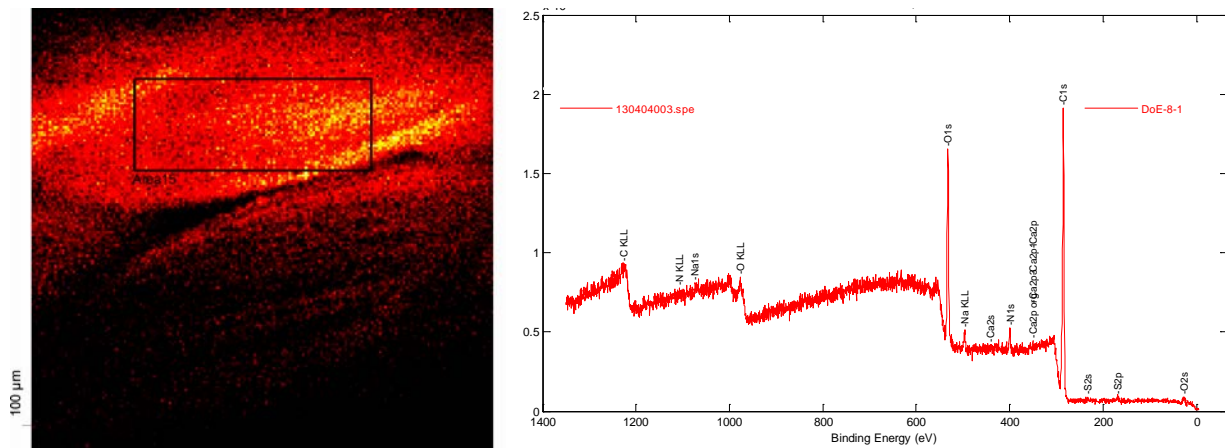


Figure 9: Left: measurement area of the XPS; right: corresponding spectrum of sample DoE-8.

The left hand side of Figure 9 shows the measurement area of the XPS: visible are the two plies of the cord, where one ply is the brighter area on the top and the other one is the darker spot below. On the right hand side is the corresponding spectrum of the sample shown, which is a plot of the peak intensity over the binding energy (eV).

In Table V the results are listed. There is a change in nitrogen (N) content visible for the DoE samples, which is an indication that a coating layer is indeed deposited. DoE-16, the sample with the most intense plasma settings, has an increased carbon (C) and nitrogen (N) content, while having the lowest oxygen (O) content. However, the differences between the DoE samples are rather small. Overall, the results show that there is a change in the chemical composition of the surface, but conclusion about the degree of coverage and thickness of the layer and type of moieties cannot be made.

**TABLE V**  
**RESULTS OF THE XPS MEASUREMENTS**

| <b>Sample</b> | <b>Description</b>              | <b>C</b> | <b>N</b> | <b>O</b> |
|---------------|---------------------------------|----------|----------|----------|
| Reference     | No treatment                    | 80.23    | 1.06     | 17.36    |
| DoE-16        | Strong plasma<br>High flow rate | 81.26    | 1.78     | 16.25    |
| DoE-8         | Strong plasma<br>Low flow rate  | 80.13    | 2.16     | 16.67    |
| DoE-9         | Weak plasma<br>High flow rate   | 80.01    | 2.18     | 17.24    |
| Doe-1         | Weak plasma<br>Low flow rate    | 80.53    | 1.97     | 16.91    |

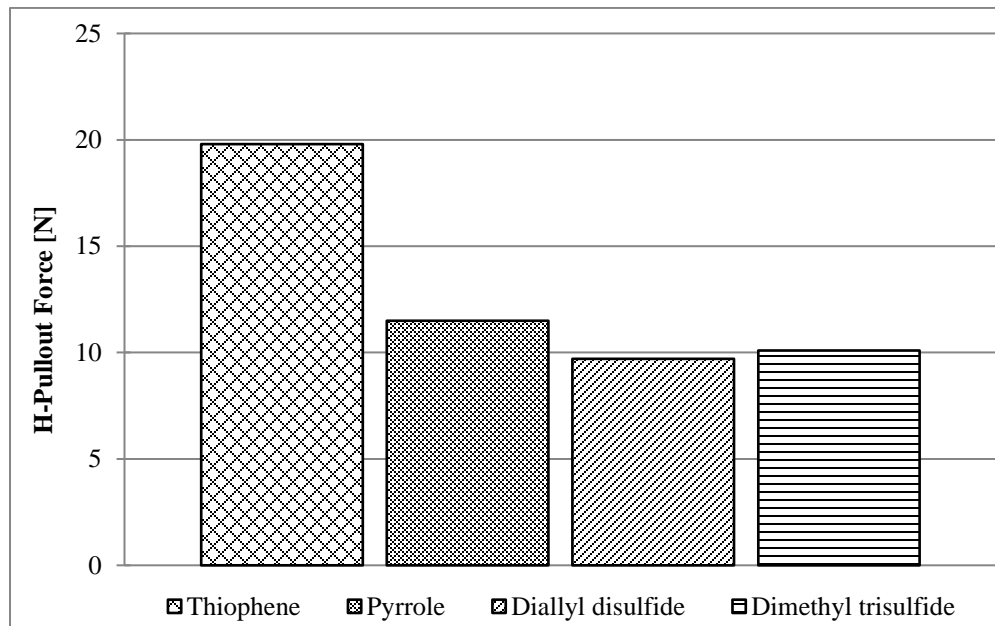


Figure 10: Comparison of thiophene, pyrrole, disulfide as well as trisulfide precursors

Figure 10 shows a comparison of different precursors applied under identical, but not optimized treatment conditions; only the evaporator temperature setting was adapted to the corresponding precursor evaporation temperature. Under these conditions, thiophene as precursor resulted in the best adhesion values. However, the absolute values are rather low, and another possible explanation besides the fact that the process conditions were not optimized might be that the interactions with the surrounding air after the actual plasma treatment can cause a passivation of the cord surface. This would require a protective atmosphere that prevents any interaction of the cord until the next reaction step is happening. To establish this, the plasma treatment chamber was adjusted for a slight overpressure of an inert gas to avoid contamination by air molecules. This enhances greatly the control over the treatment conditions during the plasma treatment process. To further protect the cord after the plasma treatment, the protective atmosphere is maintained until the cord enters the crosshead of the extruder, where it gets immediately rubberized.

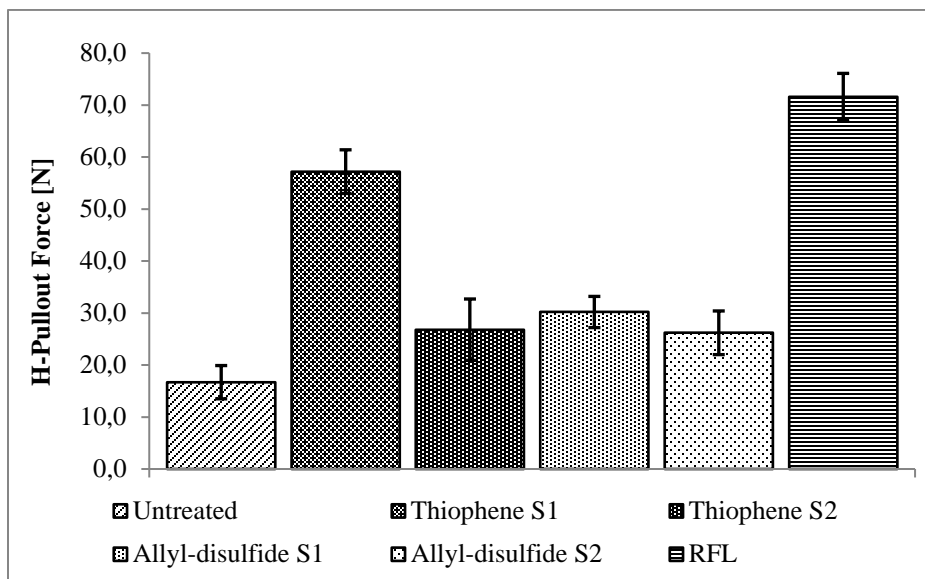


Figure 11: H-Pullout forces measured after the introduction of a protective atmosphere

Figure 11 shows, that the concept of a protective nitrogen atmosphere with immediate rubberization enhanced the adhesion force significantly. Again thiophene as precursor exhibits its clear potential, here in a comparison to diallyl disulfide: the adhesion of rayon improved by a factor of three with thiophene as precursor. The figure also illustrates a strong influence of the plasma settings, as experiments were done with full generator power (index S1) and reduced generator power (index S2). In both cases, the full power setting S1 enhanced the adhesion, in case of thiophene it had a significant effect. Besides the cords treated with the two precursors, also the untreated rayon and a RFL treated cord are shown. The adhesion of RFL treated cords is not yet reached, but the results with thiophene are very encouraging.

The strong difference caused by the plasma settings for thiophene imply, that chemical bonds are responsible for the good adhesion values in case of S1 settings. For both settings, S1 and S2, the precursor flow-rate is similar, therefore the difference of both variants is the efficiency of deposition. Apparently, the S1 type deposition allows - caused by the stronger plasma power - a more efficient plasma polymerization of thiophene. The polymeric layer formed under these plasma conditions is able to react with the sulfur complexes during the vulcanization process. From the precursors used in this study, only thiophene enhanced the adhesion significantly. A look at its molecular structure shows three features, which in synergy explain the enhancement. These properties are:



- a five membered ring-structure of the molecule,
- two double bonds, and
- one sulfur atom.

The importance of the ring-structure of thiophene is shown by the comparison with diallyl disulfide: this specific structure keeps the precursor relatively stable in the plasma compared to diallyl disulfide with double bonds and sulfur atoms, but lacking the ring-structure. An explanation might be, that the diallyl disulfide molecule gets atomized in the plasma and it therefore is not able to polymerize in a similar way as thiophene does. To elucidate the relevance of the double bonds within the molecule, a comparison of thiophene with tetrahydro-thiophene was done. The latter one is the saturated analogue of thiophene and the perfect candidate to determine which influence the double bonds of thiophene have on the adhesion.

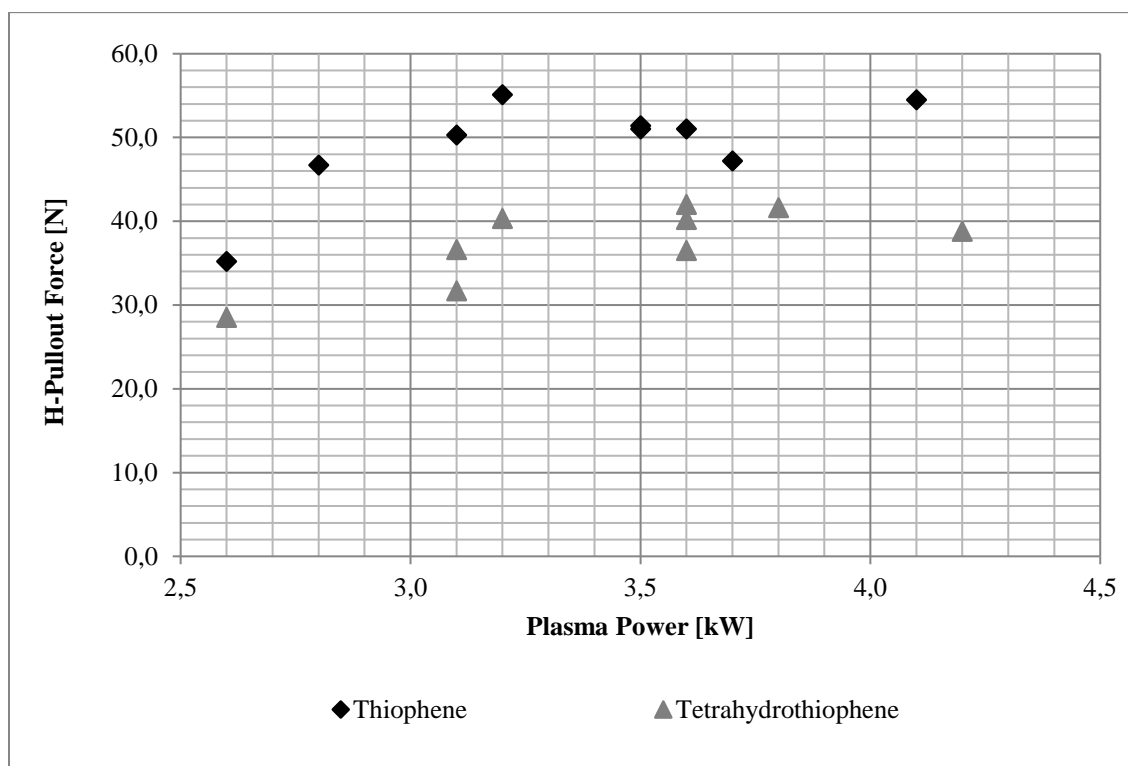


Figure 12: Adhesion values of rayon treated with thiophene and tetrahydrothiophene

In Figure 12, the adhesion values of rayon treated with the two different precursors using different plasma power settings are plotted. A plasma coating with thiophene results in higher adhesion values than the treatment with the saturated molecule. The double bonds are a clear factor

for adhesion promotion, as they are beneficial for the plasma polymerization process which leads to a better polymer coating. The plasma power settings do influence the adhesion values to a certain degree, but as the improvement with higher power settings is rather limited and scattered, this is not expected to be a major influencing factor.

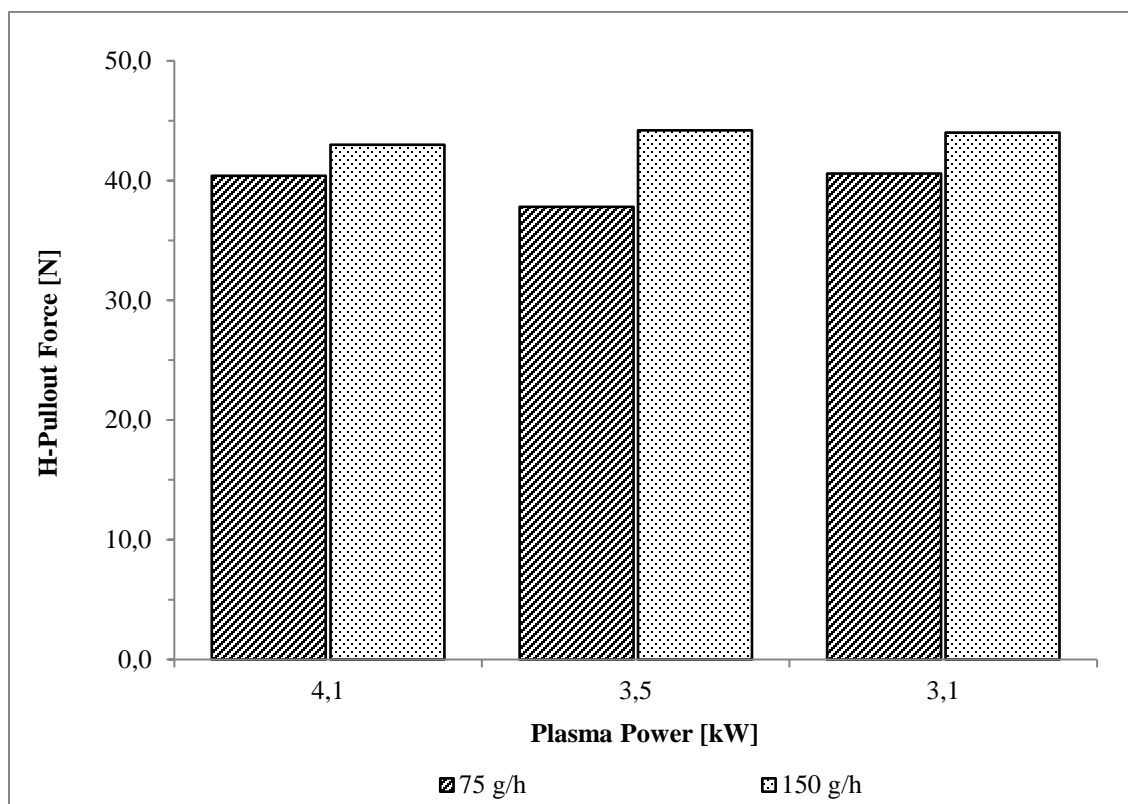


Figure 13: Influence of the precursor flow rate at different plasma power settings

Further tests with thiophene and different flow rates as well as generator settings (Figure 13) were performed to determine where the optimum of these parameters lies. While a certain benefit of a higher flow-rate is detectable, the increase of plasma power again is not conclusive. However, the overall adhesion strength in this series is lower than the values shown in Figure 12. As this series of experiments was done continuously, this lead to the conclusion that the efficiency of the plasma treatment reduces over time. An explanation for this phenomenon is, that over time more and more exhaust gases from the plasma treatment process are congested in the plasma reactor. This is caused by the slight overpressure used to create an inert atmosphere. While at the beginning of the treatment a nitrogen filled reactor chamber is present, these conditions change

with the ongoing treatment. To verify this hypothesis, a dedicated test was done, where no changes to the settings over a period of time were done. Every two minutes a sample was taken, which was afterwards tested with H-pullout tests.

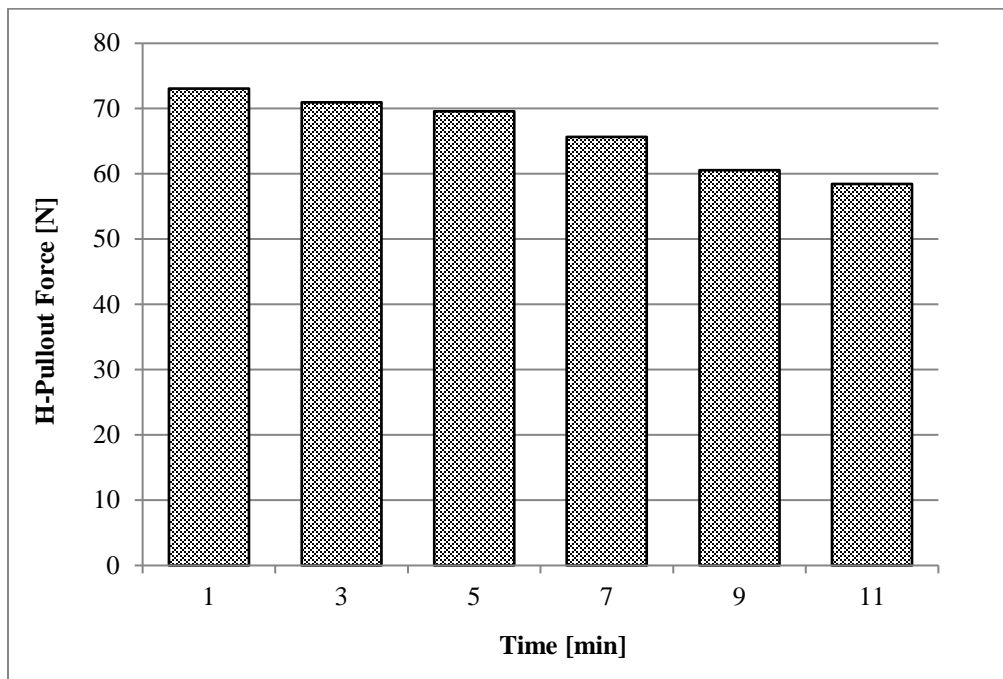


Figure 14: Decrease in H-pullout force during a long-lasting plasma treatment

The results are shown in Figure 14: clearly, a negative effect is measurable over time. This indicates that it is crucial to remove non-reacted plasma gases and to provide a constant flow of protective gas.

The third factor was the sulfur atom that is present in thiophene and is absent in pyrrole, as it is the analog molecule to thiophene with a nitrogen atom instead. Pyrrole has the ability to plasma polymerize in a similar way as thiophene does. Therefore, it is expected that the coated layers of both precursors have a similar structure.

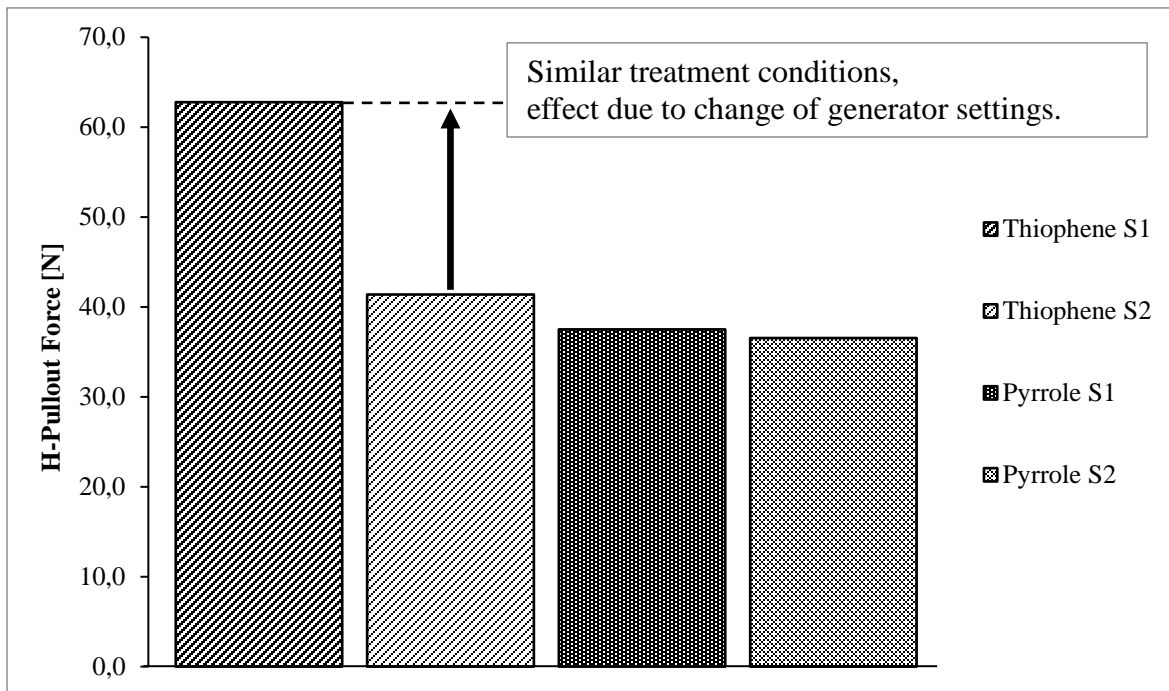


Figure 15: Effect of the presence of sulfur versus nitrogen in the precursor molecule

Figure 15 shows that the thiophene coating with a maximum plasma power of 4,1 kW generates the best adhesion values with H-pullout values of 62,8 N. When pyrrole is used under the same conditions, the effect is much less. However, using settings S2 with a reduced generator power, the adhesion values for both samples are rather low. From this can be concluded, that the presence of sulfur in the molecule structure does matter for adhesion promotion, and that the generator power has to be high enough for an efficient activation of the precursor gas.

In Figure 16, a direct comparison of a thiophene plasma coated rayon cord with its untreated equivalent shows, how strong the effect of plasma treatment on the adhesion is. Up to an elongation of about 100 % strain, the plasma treated cord can take the load stress, with a peak of ca 70 N. Then the sample fails and the measured force drops down to 40 N. At a strain of 150 %, another less significant drop down to 30 N happens. At even higher strains, the cord simply slips out of the remaining rubber with a wave-like pattern. This effect is observed for the untreated cord over the whole strain range: without treatment, the cord has no interaction at all with the rubber. The strong adhesion of the thiophene coated cord is a strong indication that the type of adhesion created by the plasma treatment is indeed based on a chemical bond.

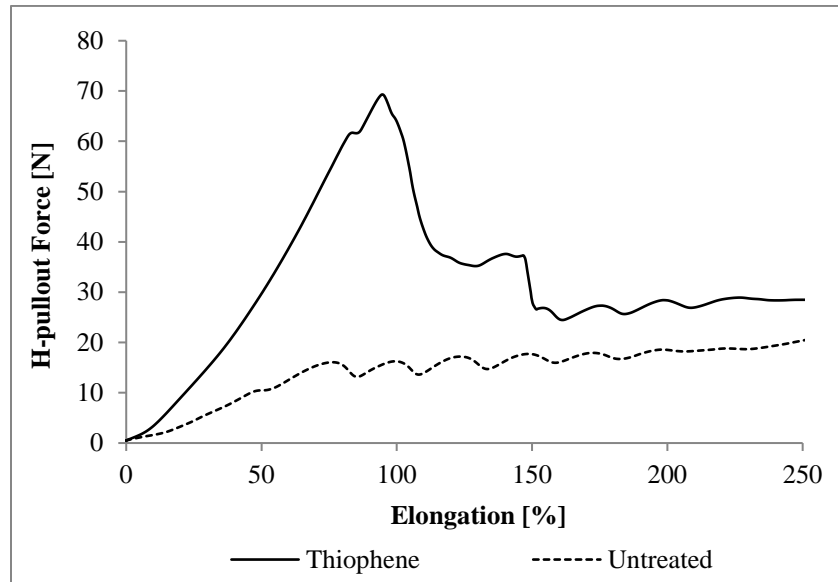


Figure 16: Force-elongation diagram of a plasma coated and an untreated cord

The conclusion that the adhesion is of chemical nature can be further strengthened with microscopic images of the tested H-pullout samples. The part of the sample where the cord was pulled out was cut in half and analyzed under an optical microscope. In the image in Figure 17, a H-pullout sample after testing with a thiophene plasma coating is shown. A significant number of filaments of the rayon cord do adhere to the rubber. This is a strong indication that the area of failure is located in the very top layer of the cord surface and not in the rubber-fiber bond. Apparently, the outer filaments of the cord break and this is where the specimen fails. This type of failure is in contrast with the untreated samples, where no filaments remain on the rubber surface and the samples fail at much lower forces during the adhesion test. However, cohesive break in the rubber was not observed.

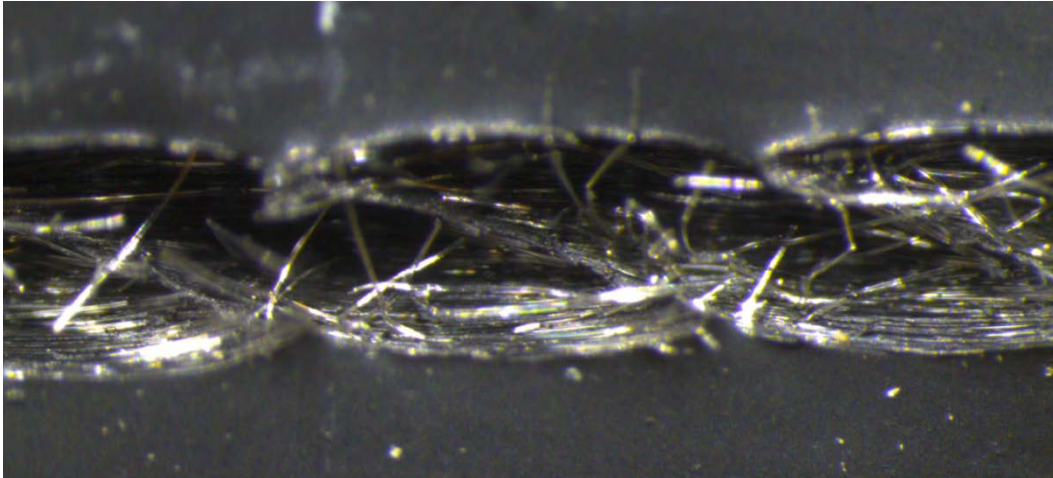


Figure 17: Filaments in a H-pullout rubber block after the pullout test

To better understand the importance of each plasma treatment step, a number of tests was performed with different combinations of treatment steps. The results are shown in Figure 18. Besides the different combinations of plasma treatments, the test conditions remained unchanged.

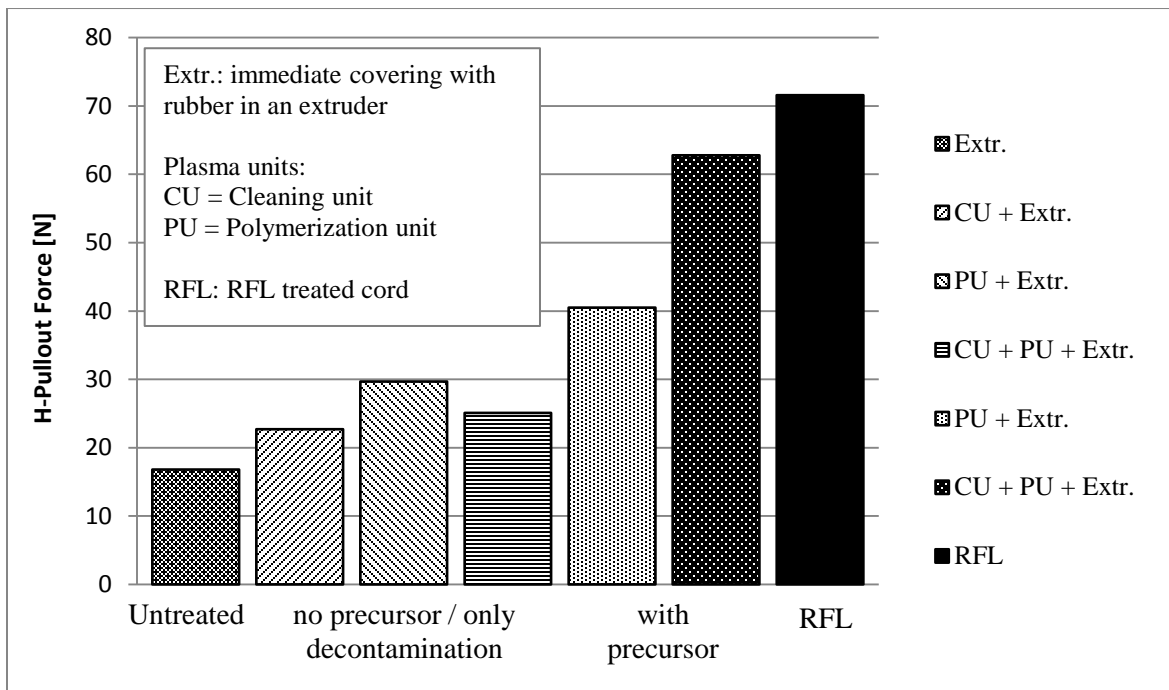


Figure 18: Effect of different treatment steps on the adhesion

On the left hand side, the untreated reference is shown, which has the lowest adhesion value. This leads to the general conclusion, that all plasma treatment steps do contribute to the adhesion

improvement. However, the effect of a decontamination - either a single treatment (CU + Extr., PU + Extr.) or the combined one (CU + PU + Extr.) - is limited to an adhesion increase factor of less than 2. If the PU unit deposits a thiophene plasma coating without prior cleaning (PU + Extr.), the adhesion improves by a factor of more than two. The by far best adhesion results are gained when the full plasma treatment is used (Cu + PU + Extr.), which proves that both steps, cleaning and plasma coating, are necessary. This results in a significant increase in adhesion, though the strength of the RFL coating is not yet reached.

Plasma activated molecule fragments are known to have a short lifespan, therefore the effect of an immediate rubberizing of the plasma coated cords was studied. The results are shown in Figure 19: the non-rubberized, unprotected sample exhibits the lowest adhesion value in this series. This shows, that the immediate protection after the plasma treatment by a rubber-layer is even more important than a decontamination prior the actual plasma treatment.

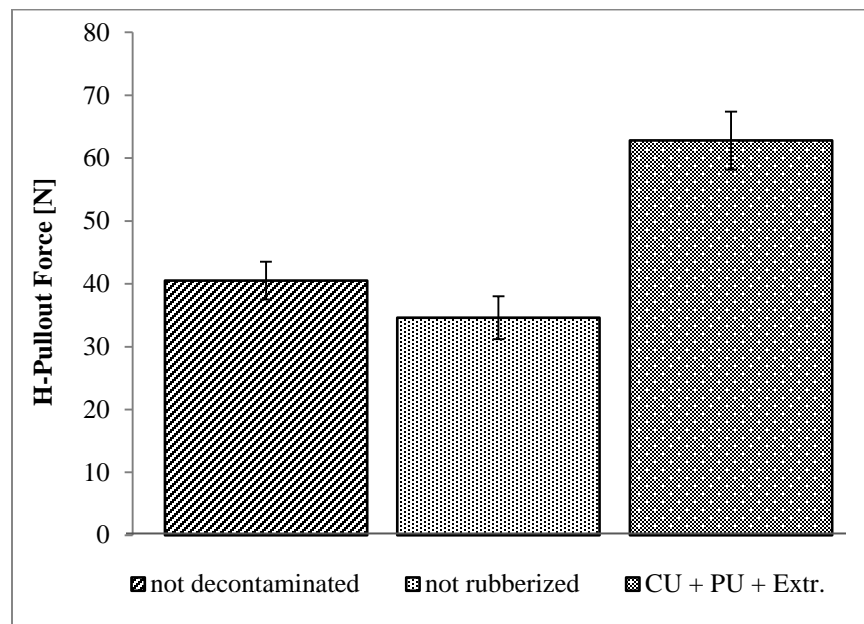


Figure 19: Effect of immediate rubber coating of the cord

The variation of the flow-rate of the precursor under improved and constant plasma conditions shows that a flow-rate of 50 g/h results in a much lower adhesion force of about 43 N than the higher flow-rates (Fig. 20). The difference between 100 and 150 g/h is less significant, but is clearly measurable as an average of 15 specimens for each test.

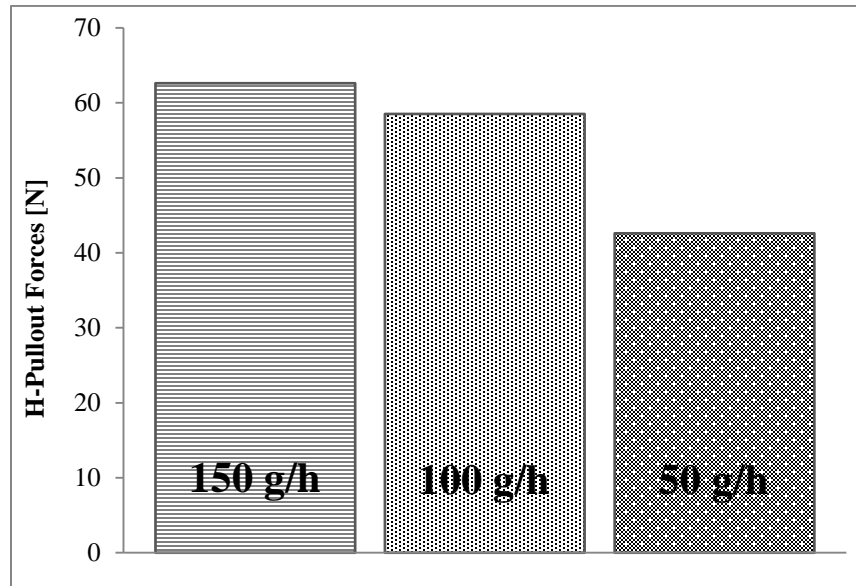


Figure 20: Effect of precursor flow-rate

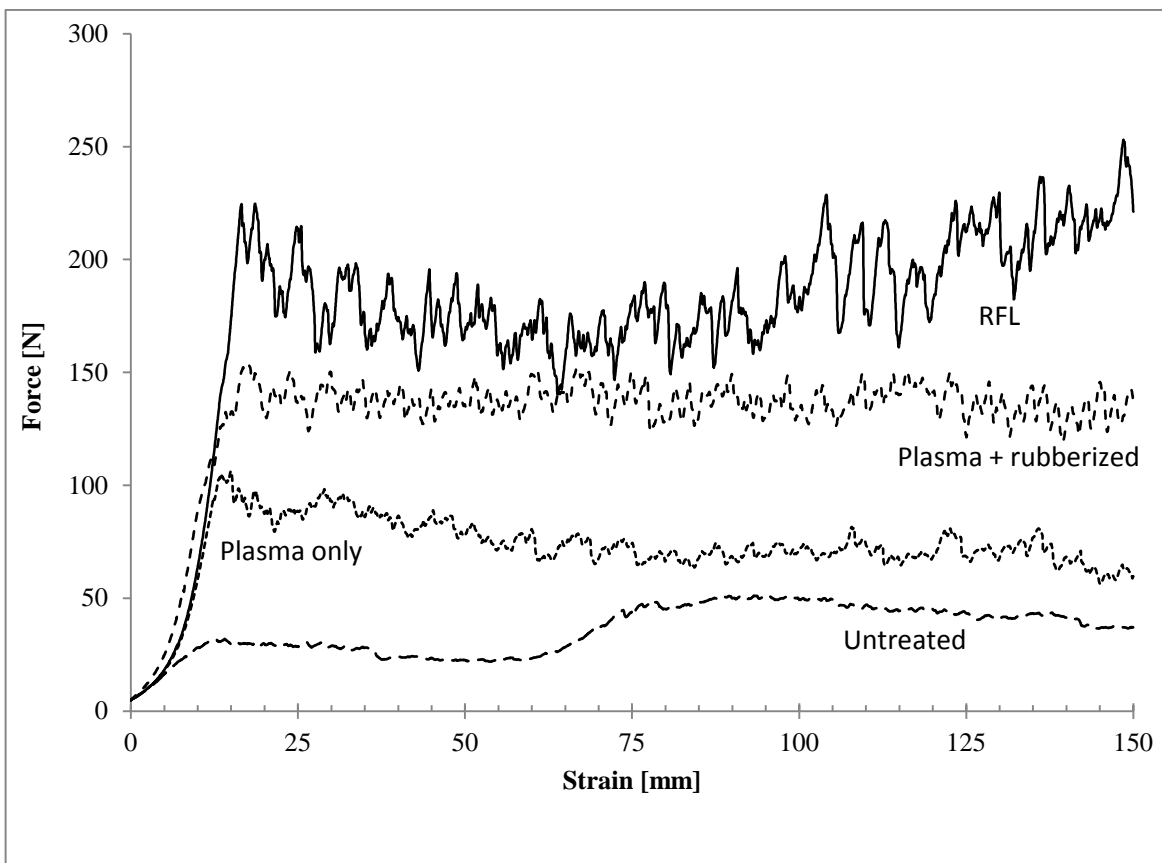


Figure 21: Results of the SPAF test of differently treated cord samples



In order to verify these results, Strap Peel Adhesion Force (SPAF) tests were performed. This test is evaluated in two ways: on the one hand a force-strain diagram is analyzed, where the forces at a strain of 30 % and 100 % are taken as comparative values. On the other hand, the sample is optically assessed and a rating is given based on how much cord is covered by rubber. Basically, this means that the amount of visible interface failure is used to depreciate the rating of the sample. The more cord is visible, the lower the rating will be.

In Figure 21, a force versus strain curve received from the SPAF test is shown. There are 4 different samples: an RFL coated sample is taken as reference, both plasma samples have a thiophene coating, but one received a rubber coating directly after the plasma coating step (plasma + rubberized), the other one not (plasma only). Finally, an untreated cord is taken as additional reference point. The RFL coating exhibits the highest forces and the most distinctive jitter effect. The jitter is generated due to the high stress that is occurring within the composite during the test. The higher the stress, the more distinctive the jitter will be. In case of the RFL sample, the failure is almost entirely on the rubber side. Only a few spots are detectable which indicate a failure in the cord-rubber-interface (Figure 22).

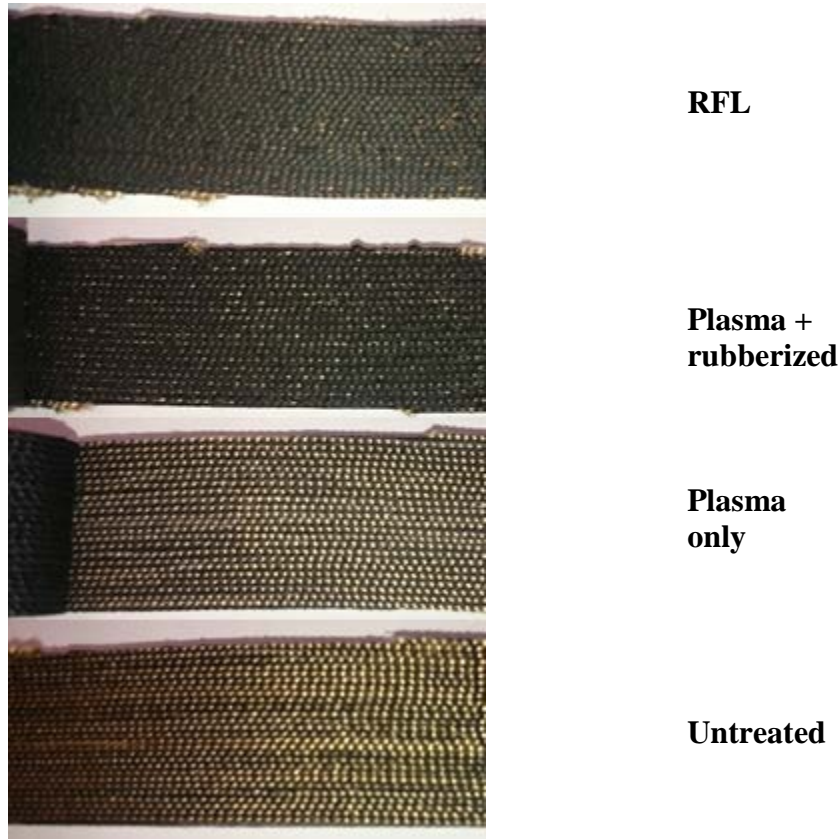


Figure 22: Samples of the SPAF test after testing to evaluate the failure interface

In contrast to the RFL-treated sample, the plasma-treated specimen show a steady force level that doesn't change during the test. The jitter is less distinctive compared to the RFL sample. Important is that the overall performance of the plasma treated and rubberized sample is even closer to the RFL reference than seen with the H-pullout test. Nevertheless, the trend seen in both tests is identical. The optical judgement of the plasma treated and rubberized specimens unfold a different picture than the force-strain diagram. A significant amount of cord is visible at the failure interface, clearly indicating that the samples tend to fail at the cord-rubber interface: they show adhesive break. Even though the measured performance is reasonably good, the type of failure is not the desired one. Possible reasons for this failure might be an insufficient penetration of the rubber into the cord.

The non-rubberized plasma sample performs clearly inferior to the rubberized one. This is true for both categories, the mechanical measurement and the optical judgement. The adhesion between cord and rubber is less and, therefore, the primary failure mode is adhesive: failure at the cord-rubber interface. This is also visible for the jitter, which is much less concise. The forces

generated by the test cannot be transferred to the cord and that prevents higher stresses in the composite.

The untreated cord is entirely unable to transfer forces and has no jitter at all. There is no reinforcing effect measurable and as a matter of fact, no adhesion between cord and rubber detectable. This can also be seen in Figure 22 (untreated), which unveils a complete interface failure.

## CONCLUSIONS

In this study, adhesion between rayon cords and rubber could be achieved by a two-step plasma treatment. The most promising precursor for this purpose was found to be thiophene. While the improvement was significant, it however did not reach the level of RFL-coated cords. Besides, the failure mode was different: In the case of RFL treatment, cohesive failure occurred, thus mainly in the rubber phase. In the case of plasma treated cords, the outer filaments of the cords failed first when a load was applied. The filaments remaining in the rubber phase can be seen as an evidence of chemical adhesion.

The requirements for the plasma precursor for adhesion promotion of rayon cord to rubber were defined. Experiments with different sulfuric precursors showed clearly, that thiophene was the only one able to significantly improve cord-rubber adhesion. Its unique characteristic property over the other precursors is the ring-structure, which stabilizes the molecule so that its functionalities remain intact while exposed to the plasma. As a consequence, the created polymeric layer has much more repeating units with a significantly higher number of functional groups compared to the other precursors, resulting in the ability to create a significantly higher level of adhesion.

A comparison of thiophene with pyrrole, which has a similar molecule structure in which the sulfur atom of the thiophene is substituted by a secondary amine in case of pyrrole, indicated the importance of a sulfur atom in the ring. While thiophene performed well, pyrrole could enhance the adhesion level only slightly. Clearly, the sulfur atom of thiophene helps with the interaction of the plasma polymerized layer with the formed sulfur complexes during vulcanization.

Another comparison of thiophene with tetrahydrothiophene further underlined the importance of double bonds in the ring structure, which are entirely absent in case of

tetrahydrothiophene. This causes a less stable ring which probably gets cracked during exposure to the plasma and prevents a similar plasma polymerization like thiophene undergoes.

Besides those requirements for the precursor molecule, it is evident that the plasma treatment takes place in a protective atmosphere like nitrogen. It is not only important to use nitrogen as ionization gas, but also to create a protective atmosphere around the cord until it gets in touch with rubber.

#### ACKNOWLEDGEMENTS

This project was fully financed and technically supported by VMI Holland BV in Epe, The Netherlands.

#### REFERENCES

- [1] [http://www.wiredchemist.com/chemistry/data/bond\\_energies\\_lengths.html](http://www.wiredchemist.com/chemistry/data/bond_energies_lengths.html), accessed 18.08.2017.
- [2] R.A. Jones (ed.), *The Chemistry of Heterocyclic Compounds, Pyrroles*. Wiley, Hoboken, United States, 1990, ch. 1, p. 5.
- [3] V.S. Shanthalaa,\*, S.N. Shobha Devib, and M.V. Murugendrappaca, *J. Asian Ceramic Soc.* Available online: <http://dx.doi.org/10.1016/j.jascer.2017.02.005>.
- [4] M. Dahlmann, J. Grub, and E. Löser, Butadiene, in *Ullmann's Encyclopedia of Industrial Chemistry*, Wiley-VCH, Weinheim, Germany, 2011, p. 1-24.
- [5] H.K. Yasuda, *Plasma Polymerization*, Academic Press, London, Great Britain, 1985.
- [6] R. Shishoo, *Plasma Technologies for Textiles*. Woodhead Publishing, Sawston, Great Britain, 2007.
- [7] ASTM Standard *ASTM D4776 / D4776M-10*, "Standard Test Method for Adhesion of Tire Cords and Other Reinforcing Cords to Rubber Compounds by H-Test Procedure" *Annu. Book ASTM Stand.* **07.02**, (2010).
- [8] ASTM Standard *D4393-00*, "Standard Test Method for Strap Peel Adhesion of Reinforcing Cords or Fabrics to Rubber Compounds" *Annu. Book ASTM Stand.* **13.19**, (2000).
- [9] G.J. Cruz, J. Morales, and R. Olayo, *Thin Solid Films*, **342**(1-2), 119 (1999).

**TABLE VI**  
**OVERVIEW OF THE PROPERTIES OF SULFUR PRECURSORS**

| <b>Precursor</b>                 | <b>Thiophene</b>                | <b>Diallyl disulfide</b>                      | <b>Dibenzyl disulfide</b>                      | <b>Dimethyl trisulfide</b>                   |
|----------------------------------|---------------------------------|---|--|--|
| <b>Molecular Formula</b>         | C <sub>4</sub> H <sub>4</sub> S | C <sub>6</sub> H <sub>10</sub> S <sub>2</sub> | C <sub>14</sub> H <sub>14</sub> S <sub>2</sub> | C <sub>2</sub> H <sub>6</sub> S <sub>3</sub> |
| <b>CAS number</b>                | 110-02-1                        | 2179-57-9                                     | 150-60-7                                       | 3658-80-8                                    |
| <b>Molecular weight, g/mol</b>   | 84,14                           | 146,28  | 246,39   | 126,26                                       |
| <b>Density, g/cm<sup>3</sup></b> | 1,06                            | 1,01  | 1,30   | 1,20   |
| <b>Melting point, °C</b>         | -38                             | 79*   | 69-72  | -68  |
| <b>Boiling point, °C</b>         | 84                              | 180   | 210-216  | 170  |
| <b>Hazard symbol</b>             | F, Xn                           | Xn  | Xi   | none   |

\*at 16 mm Hg

**TABLE VII**  
**BOND ENERGIES OF COMMON CARBON AND SULFUR BONDS [1]**

| <b>Bond</b>                | <b>kJ/mol</b> | <b>eV</b> | <b>Bond</b> | <b>kJ/mol</b> | <b>eV</b> |
|----------------------------|---------------|-----------|-------------|---------------|-----------|
| <b>C-C</b>                 | 346           | 3.6       | <b>C=C</b>  | 602           | 6.3       |
| <b>C-O</b>                 | 358           | 3.7       | <b>C=O</b>  | 799           | 8.3       |
| <b>C-S</b>                 | 272           | 2.8       | <b>C=S</b>  | 573           | 6.0       |
| <b>S-S (S<sub>8</sub>)</b> | 226           | 2.3       | <b>S=S</b>  | 425           | 4.4       |
| <b>C-N</b>                 | 305           | 3.2       | <b>C=N</b>  | 615           | 6.4       |

**TABLE VIII**  
**SELECTED PLASMA PARAMETERS FOR THE DOE TRIALS**

| <b>Factor</b> | <b>Type</b>     | <b>-</b> | <b>+</b> | <b>CP</b> |
|---------------|-----------------|----------|----------|-----------|
| <b>A</b>      | Voltage [%]     | 85       | 100      | 92,5      |
| <b>B</b>      | Frequency [kHz] | 19       | 25       | 22        |
| <b>C</b>      | Cycle time [%]  | 50       | 100      | 75        |
| <b>D</b>      | Flow-Rate [g/h] | 20       | 100      | 60        |

**TABLE IX**  
**THE DOE SETUP**

| #DoE- | A | B | C | D | Answer |
|-------|---|---|---|---|--------|
| 1     | - | - | - | - | 9,3    |
| 2     | + | - | - | - | 10,4   |
| 3*    | - | + | - | - | -      |
| 4*    | + | + | - | - | -      |
| 5     | - | - | + | - | 9,8    |
| 6     | + | - | + | - | 9,5    |
| 7*    | - | + | + | - | -      |
| 8     | + | + | + | - | 10,1   |
| 9     | - | - | - | + | 9,5    |
| 10    | + | - | - | + | 9,3    |
| 11*   | - | + | - | + | -      |
| 12*   | + | + | - | + | -      |
| 13    | - | - | + | + | 9,8    |
| 14    | + | - | + | + | 10,9   |
| 15    | - | + | + | + | 11,2   |
| 16    | + | + | + | + | 11,6   |
| CP    | 0 | 0 | 0 | 0 | 11,1   |

*\* These parameter settings that did not allow plasma ignition*



**TABLE X**  
**RESULTS OF THE XPS MEASUREMENTS**

| <b>Sample</b> | <b>Description</b>              | <b>C</b> | <b>N</b> | <b>O</b> |
|---------------|---------------------------------|----------|----------|----------|
| Reference     | No treatment                    | 80.23    | 1.06     | 17.36    |
| DoE-16        | Strong plasma<br>High flow rate | 81.26    | 1.78     | 16.25    |
| DoE-8         | Strong plasma<br>Low flow rate  | 80.13    | 2.16     | 16.67    |
| DoE-9         | Weak plasma<br>High flow rate   | 80.01    | 2.18     | 17.24    |
| Doe-1         | Weak plasma<br>Low flow rate    | 80.53    | 1.97     | 16.91    |

Figure 23: Thiophene  
Figure 24: Diallyl disulfide  
Figure 25: Dibenzyl disulfide  
Figure 26: Dimethyl trisulfide  
Figure 27: Pyrrole  
Figure 28: 1,3-butadiene  
Figure 29: Tetrahydrothiophene  
Figure 30: Final CAD design of the overpressure plasma chamber with the four APPJs in place  
Figure 31: Left: measurement area of the XPS; right: corresponding spectrum of sample DoE-8  
Figure 32: Comparison of thiophene, pyrrole, a disulfide as well as a trisulfide as precursors  
Figure 33: H-Pullout forces measured after the introduction of a protective atmosphere  
Figure 34: Adhesion values of rayon treated with thiophene and tetrahydrothiophene  
Figure 35: Influence of the precursor flow rate at different plasma power settings  
Figure 36: Decrease in H-pullout force during a long-lasting plasma treatment  
Figure 37: Effect of the presence of sulfur versus nitrogen in the precursor molecule  
Figure 38: Force-elongation diagram of a plasma coated and an untreated cord.  
Figure 39: Filaments in a H-pullout rubber block after the test  
Figure 40: Effect of immediate rubber coating of the cord  
Figure 41: Effect of precursor flow-rate  
Figure 42: Results of the SPAF test of differently treated cord samples  
Figure 43: Samples of the SPAF test after testing to evaluate the failure interface